Surface Structure of Ultrathin Fe Films on Cu(001) Revisited

T. Bernhard, M. Baron, M. Gruyters, and H. Winter*

Institut für Physik, Humboldt Universität zu Berlin, Newtonstrasse 15, D-12489 Berlin-Adlershof, Germany

(Received 24 May 2005; published 18 August 2005)

The structure and magnetism of ultrathin Fe films epitaxially grown on a Cu(001) surface are investigated by grazing scattering of fast H and He atoms or ions. By making use of a new variant of ion beam triangulation based on the detection of the number of emitted electrons, we obtain direct information on the structure of the film surface. We observe for room temperature growth a dominant and defined fcc-like structure. Complex surface reconstructions as reported in recent STM and LEED studies are observed only for cooling and H_2 dosing.

DOI: 10.1103/PhysRevLett.95.087601 PACS numbers: 79.20.Rf, 68.55.−a, 75.70.−i

The structural and magnetic properties of ultrathin Fe films epitaxially grown on a Cu(001) surface have been the subject of intense research for more than a decade, motivated by interesting features caused by the reduced dimensionality. In the bulk, Fe crystallizes in a ferromagnetic body-centered cubic (bcc) structure (α-Fe) and above 1185 K exists a face-centered cubic (fcc) phase (γ-Fe). A possibility for the stabilization of the latter phase at room temperature is epitaxial growth on fcc substrates as Cu(001) where the close matching of lattice constants of Cu ($a_{\mathrm{Cu}} = 3.615$ Å) and fcc Fe ($a_{\mathrm{Fe\text{-}fcc}} = 3.58$ Å) favors stress-free growth.

In early work, three different regimes have been identified concerning structural and magnetic properties for growth at room temperature [1–5]. For coverage up to about 4 monolayers (ML) a ferromagnetic (FM) phase with direction of magnetization normal to the film plane (''regime RT I''), followed up to about 10 ML by a FM ''live layer'' with normal magnetization on top of an antiferromagnetic stack (''regime RT II''). In both regimes a defined layer-by-layer growth takes place where a fcc-like structure of the film was considered. At even higher coverages, a transition from fcc to bcc phase takes place accompanied by a change of the magnetization axis into the plane (''regime RT III''). Our studies on growth and in-plane magnetization for Fe/Cu(001) outlined below are in full accord with this scheme.

Recently, investigations based primarily on scanning tunneling microscopy (STM) have challenged the structural model of a fcc-like Fe film in regimes RT I and RT II [6–9]. For growth at room temperature and data recorded at cryogenic temperatures it was concluded that the local atomic arrangement is related to the native bcc α-Fe structure and that one has to discard the concept of the existence of ferromagnetic γ-Fe films on Cu(001). These findings found support from local spin density calculations concluding that tetragonally distorted γ-Fe is unstable with respect to shear transformation [10]. These structures are consistent with detailed LEED work [8,11].

In this Letter we present measurements performed with a new variant of ion beam triangulation [12], which provide evidence for the dominance of a fcc(001) surface structure in the regimes RT I and RT II. This is in accord with previous structural models established about a decade ago. By cooling of the films and controlled adsorption of hydrogen, we find surface reconstructions as reported in recent STM and LEED studies. However, these structures are not present for growth *and* instant measurement at room temperature.

The experiments were performed in an ultrahigh vacuum chamber at a base pressure of some 10^{-11} mbar. Well collimated beams of H and He atoms or ions with energies from 25 to 29 keV are scattered under a grazing of incidence $\Phi_{\mathrm{in}} \approx 1.6°$ from a clean and flat Cu(001) surface on which Fe films are grown via molecular beam epitaxy at typical rates of 0.3 ML/min. Owing to the extreme projection of the beam diameter onto the surface, the data result from a spatial averaging of typically mm. Growth is inspected via the intensity of specularly reflected fast He atoms, which is closely related to surface morphology [13–15]. For layer-by-layer growth, maxima in the periodic behavior correspond to the smooth surface of completed surface layers. In Fig. 1 we show the intensity of reflected 25 keV He atoms as a function of Fe coverage of the Cu(001) substrate at temperature $T_{\mathrm{gr}} = 300$ K (RT, upper panel) and $T_{\mathrm{gr}} = 190$ K (LT, lower panel). At RT, we observe from 2 ML up to about 10 ML defined oscillations that reflect good layer-by-layer growth. For higher coverages, the drop in intensity indicates an increased roughness of the film. We reveal from Auger electrons induced by grazing impact of 29 keV protons (high surface sensitivity [16]) that early growth is affected by intermixing processes (about 20% Cu in the first layer). For 190 K we observe layer-by-layer growth up to about 4 ML and an increase of island densities for higher coverage. From the maxima of curves shown in Fig. 1 we derive the film thickness to a tenth of a ML.

Our results are in accord with previous studies on growth for this system [1,3,5] and demonstrate comparable experimental conditions. The designations ''RT I, RT II, RT III'' as well as ''LT I, LT II'' were introduced in past studies and are closely related to the magnetic properties of

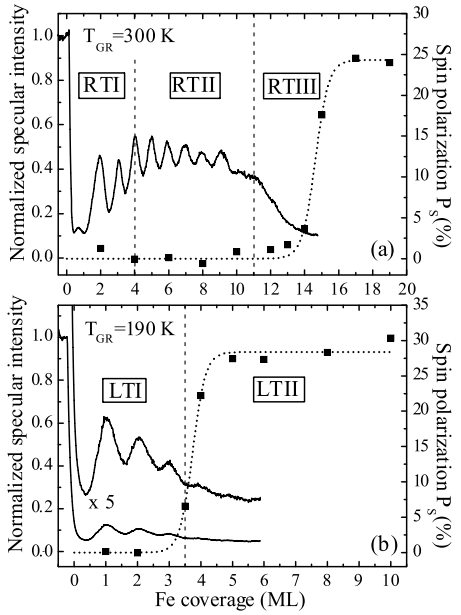

FIG. 1. Normalized intensity of reflected He atoms (solid lines; left scales) and remanent spin polarization P_S from electron capture (squares; right scales) with increasing deposition of Fe on Cu(001) at $T_{\mathrm{GR}} = 300$ K (top) and $T_{\mathrm{GR}} = 190$ K (bottom). Dotted lines are drawn to guide eyes. Vertical dashed lines separate different regimes described in text.

Fe/Cu(001). The in-plane magnetic properties of the film were studied by the capture of spin-polarized electrons into excited atomic terms where the circular polarization of the emitted light is related to the electronic spin polarization P_S and the long-range magnetic order in the topmost layer of the surface [17,18]. We investigated light emitted in the He I $2s\,^3S$–$3p\,^3P$, $\lambda = 388.9$ nm transition along the direction of magnetization parallel to the surface. The spin polarization P_S as a function of Fe coverage is shown as full symbols in Fig. 1. The onset at different coverages for RT and LT growth compares well with studies using the magneto-optical Kerr effect [1,2]. The onset of in-plane magnetism has been shown to be closely related to the transition from a fcc to a bcc phase. This interpretation is supported by our studies on surface structure using ion scattering.

The structure of the film surface is investigated by a new variant of ion beam triangulation [12] where electron emission is recorded for grazing scattering of fast atoms or ions with energies of some 10 keV. Whenever projectiles impinge along low-index directions in the surface plane (axial surface channeling [19]), their trajectories are substantially changed compared to the planar symmetry met for a random azimuthal orientation of the target. Then regions of higher electron densities in the surface plane and, in particular, subsurface layers are probed resulting in an enhanced number of electrons emitted per projectile. In a recent paper this feature was experimentally demonstrated by recording for impact of fast H and He atoms emitted electrons by means of a surface barrier detector (SBD) biased to a high voltage of about 25 kV [20]. The pulse height is proportional to the number of electrons emitted per scattering event and allows one to study electron number spectra (ENS) [21]. The advantages to detect electrons instead of the target current as performed in Ref. [12] are the following: (1) very low projectile dose (equivalent currents of sub-fA), (2) efficient self-normalization of data, and (3) enhanced surface sensitivity and signals (see below).

Here we apply this detection scheme with a discriminator level set to a pulse height interval equivalent from about 1 to 4 electrons emitted during scattering of 29 keV protons under $\Phi_{\mathrm{in}} = 1.6°$. The count rate is normalized to the overall detector counts. Since the maximum of the ENS at random azimuth is at about 5 electrons, i.e., slightly above the selected interval, an enhancement of the mean number of emitted electrons under axial channeling leads to a decrease of events with low electron number and of the normalized count rate. Since the change in events is triggered by the structure of the topmost surface layer, our method shows an extreme sensitivity to this region. Penetration of this layer is determined by the width between adjacent channels d_{ap} and the axial scattering potential that depends on the distance $d_{[uv]}$ between atoms of strings along $[uv]$. The indices $[uv]$ refer to low-index directions in the primitive square lattice. Since d_{ap} dominates the continuum potential for scattering of projectiles from strings of target atoms [19], the decrease of d_{ap} with increasing index $[uv]$, i.e., a narrowing of axial channels, leads to a reduced probability for penetration of the surface and a decrease of signals. Computer simulations based on classical trajectories reproduce quantitatively the disappearance of signals for higher $[uv]$.

In Fig. 2 we show normalized SBD counts as a function of azimuthal angle Θ for an increasing number of Fe ML grown at $T_{\mathrm{gr}} = 300$ K. The curves show pronounced minima, if the direction of the incident beam coincides with low-index directions of the surface lattice (data for random azimuth normalized to one). For the clean Cu(001) surface the $[uv]$ directions in the primitive square lattice with constant $a_{\mathrm{Cu}}/\sqrt{2}$ are revealed up to direction [41] (see also upper left panel of Fig. 3). The dips along [10] directions show a peaked structure because of a string in the middle of the axial channel in the second layer. The striking feature of our data is the clear-cut signature of a fcc(001) structure up to a coverage of about 10 ML where the curves change to a bcc(110)-like phase (cf. upper middle panel of Fig. 3).

Only for 3 ML we observe a reduction of peaks that can be understood from our computer simulations by the formation of a laterally distorted sinusoidal-like (5×1) structure as found in former LEED studies [4]. Contributions of a (4×1) bcc-like structure (cf. upper right panel of Fig. 3) proposed from recent LEED [2,4] and STM studies [8,9]

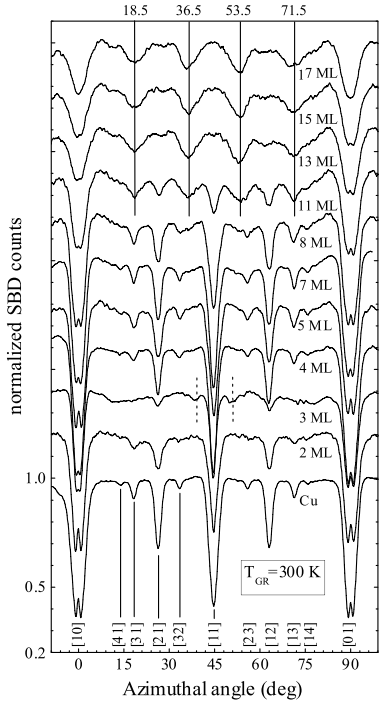

FIG. 2. Normalized SBD counts versus azimuthal angle of incidence Θ for grazing scattering of 29 keV protons from Cu(001) under $\Phi_{in} = 1.6°$ at $T_{GR} = 300$ K with increasing Fe coverage. Curves are shifted with respect to data for clean surface at bottom. Vertical lines in lower part indicate low-index directions $[uv]$ in primitive square surface lattice.

are estimated to less than 20% here. Furthermore, for about 2 and 4 ML the triangulation data are close to that for the clean substrate; i.e., the bcc phase cannot play a substantial role for the overall structure and magnetic properties of the surface.

For coverages above 10 ML, a transition to regime RT III takes place. Atomic rows with high densities are oriented along $\Theta \approx 18.5°$ ($\Theta \approx 71.5°$) and $\Theta \approx 53.5°$ ($\Theta \approx 36.5°$) with respect to the initial [10] direction of the substrate. The angles in parentheses originate from different domains with perpendicular orientation. Our measurements show a relaxed bcc(110)-like surface with an angle $\alpha \approx 71.5°$ between two primitive lattice vectors. A similar value of $\alpha \approx 72.1°$ is reported from LEED [22]. Both results are close to the ideal value $\alpha = 70.5°$ for α-Fe.

It should be noted that mainly two structural phases seem to exist. In regimes RT I and RT II a fcc(001)-like and in RT III a bcc(110)-like structure with an angle $\vartheta \approx 18.5°$ with respect to the original position in the fcc(001) lattice. The transition of structures between regimes RT II and RT III is abrupt. No intermediate angles ϑ between 0° and 18.5° are observed, which would support a gradual shearing of the fcc lattice towards the α-Fe structure. This is also indicated by the coexistence of both phases at 11 ML.

For regime RT II, LEED studies suggest a (2×1) structure [1,4]. Recent STM data show a $p4g(2 \times 2)$ reconstruction [8,9] also known as clockwork reconstruction because of clockwise and counterclockwise rotated squares, which result from a zigzag deformation (lower panel of Fig. 3). At 5 and 80 K, an angle $\alpha \approx 70°$ has been found, close to bcc(110) ($\alpha = 70.5°$). For room temperature, this structure could not be resolved by STM, which was ascribed to rapid fluctuations of domain boundaries [9].

In combined triangulation and LEED studies at room temperature, we could not observe noticeable signatures of the structures proposed recently for RT II. In order to explore the origin for this discrepancy, we cooled down the target after growth to $T = 190$ K and exposed it to H_2 at about 10^{-7} mbar. The resulting LEED pattern and triangulation curves are displayed in Fig. 4. At $T = 190$ K we observe a noticeable but still weak signature of a (2×1)

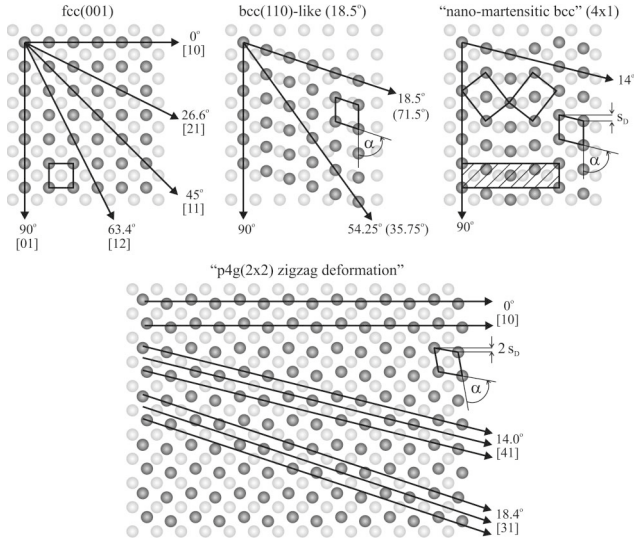

FIG. 3. Sketch of structural models for Fe/Cu(001).

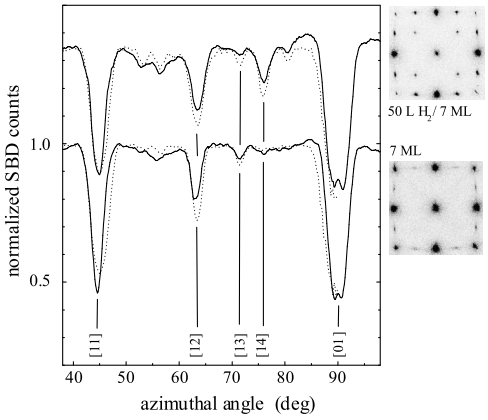

FIG. 4. Same as Fig. 2 for 7 ML films grown at 300 K and measured at 190 K. Lower curve and LEED pattern: no H_2 dose; upper curve and LEED pattern: 50 L H_2. Dotted curves: results from computer simulations.

structure that shows almost no effect on the triangulation curve for room temperature. For a H_2 dose of 50 L (1 L = 1 Langmuir = 1.33×10^{-6} mbar s) a $p4g(2 \times 2)$ structure in the LEED pattern is revealed. Concerning triangulation for a surface with the proposed $p4g(2 \times 2)$ structure, an accidental geometrical arrangement of surface atoms along the [41] direction is of relevance here. For an unreconstructed surface, such a high index channel is too narrow for penetration of the surface layer and only a weak dip can be identified (cf. Figs. 2 and 4). However, for the ''zigzag deformation'' of the reconstructed surface, atoms of neighboring channels are aligned closely along this axial direction (angle of 14° with respect to [10]) resulting in an effective opening of this channel (cf. lower panel of Fig. 3). For other channels (e.g., [31]) this shearing of the surface lattice leads to a narrowing of axial channels and a reduction of the triangulation signal.

This effect can nicely be seen in the triangulation curves shown in Fig. 4. Comparing the two data sets, we reveal that for the transition from (partial) (2×1) to $p4g(2 \times 2)$ reconstruction the dips for [41] directions are clearly enhanced, whereas the signals for scattering along [31] are reduced. This feature is reproduced in our computer simulations on a quantitative level (dotted curves in Fig. 4) [23] and allows us to detect the $p4g(2 \times 2)$ structure with high sensitivity. Therefore we clearly exclude from triangulation relevant contributions of this latter structure to films grown *and* measured in RT II. We propose that for growth of Fe on very clean and flat Cu(001) in RT II an unreconstructed fcc(001) surface is present. From our simulations we estimate contributions from $p4g(2 \times 2)$ to less than about 10%. This specific method of ion scattering provides structural information from the topmost surface layer, however, is not sensitive to vertical arrangements of atoms in the surface region. From LEED and surface x-ray reliable information on an interlayer expansion and increased atomic volume is obtained [5,8,24], consistent with ferromagnetic coupling of film atoms [25].

In conclusion, ion beam triangulation based on electron emission provides at-sight information on the structure of ultrathin Fe films grown on Cu(001). We could show at room temperature that films up to about 10 ML have an in-plane fcc(001) structure of the substrate. Our measurements at lower temperatures and for H_2 adsorption reveal reconstructions consistent with recent STM studies. However, these structures are definitely not present at room temperature. So we see no need to discard the idea of a ferromagnetic fcc-Fe for thin Fe/Cu(001) films. In future work on the long-standing structural puzzle for this system, it would be of interest to explore further details as the structural change for films about 3 ML thick.

Helpful discussions with Professor J. Kirschner (Halle) are gratefully acknowledged. This work was supported by the Deutsche Forschungsgemeinschaft (Wi 1336).

*Author to whom correspondence should be addressed.
Electronic address: winter@physik.hu-berlin.de

[1] J. Thomassen, F. May, B. Feldmann, M. Wuttig, and H. Ibach, Phys. Rev. Lett. **69**, 3831 (1992).
[2] S. Müller *et al.*, Phys. Rev. Lett. **74**, 765 (1995).
[3] J. Giergiel, J. Shen, J. Woltersdorf, A. Kirilyuk, and J. Kirschner, Phys. Rev. B **52**, 8528 (1995).
[4] K. Heinz, S. Müller, and P. Bayer, Surf. Sci. **352–354**, 942 (1996).
[5] A. Kirilyuk, J. Giergiel, J. Shen, M. Straub, and J. Kirschner, Phys. Rev. B **54**, 1050 (1996).
[6] A. Biedermann, M. Schmidt, and P. Varga, Phys. Rev. Lett. **86**, 464 (2001).
[7] A. Biedermann, R. Tscheliessnig, M. Schmidt, and P. Varga, Phys. Rev. Lett. **87**, 086103 (2001).
[8] A. Biedermann, R. Tscheliessnig, C. Klein, M. Schmidt, and P. Varga, Surf. Sci. **563**, 110 (2004).
[9] A. Biedermann, R. Tscheliessnig, M. Schmidt, and P. Varga, Appl. Phys. A **78**, 807 (2004).
[10] D. Spisak and J. Hafner, Phys. Rev. Lett. **88**, 056101 (2002).
[11] L. Hammer, S. Müller, and K. Heinz, Surf. Sci. **569**, 1 (2004).
[12] R. Pfandzelter, T. Bernhard, and H. Winter, Phys. Rev. Lett. **90**, 036102 (2003).
[13] R. Pfandzelter, Surf. Sci. **421**, 263 (1999).
[14] J. G. C. Labanda and S. A. Barnett, Appl. Phys. Lett. **70**, 2843 (1997).
[15] M. H. Langelaar and D. O. Boerma, Surf. Sci. **436**, 237 (1999).
[16] R. Pfandzelter and J. Landskron, Phys. Rev. Lett. **70**, 1279 (1993).
[17] H. Winter, H. Hagedorn, R. Zimny, H. Nienhaus, and J. Kirschner, Phys. Rev. Lett. **62**, 296 (1989).
[18] J. Leuker, H. W. Ortjohann, R. Zimny, and H. Winter, Surf. Sci. **388**, 262 (1997).
[19] D. S. Gemmell, Rev. Mod. Phys. **46**, 129 (1974).
[20] H. Winter *et al.*, Phys. Rev. B **69**, 054110 (2004).
[21] F. Aumayr, G. Lakits, and H. P. Winter, Appl. Surf. Sci. **47**, 139 (1991).
[22] M. Wuttig *et al.*, Surf. Sci. **291**, 14 (1993).
[23] M. Baron *et al.* (to be published).
[24] H. L. Meyerheim, R. Popescu, D. Sander, J. Kirschner, O. Robach, and S. Ferrer, Phys. Rev. B **71**, 035409 (2005).
[25] V. L. Moruzzi, P. M. Markus, and J. Kübler, Phys. Rev. B **39**, 6957 (1989).